Diffusion, Subdiffusion, and Trapping of Active Particles in Heterogeneous Media

Oleksandr Chepizhko[1,2] and Fernando Peruani[2,*]

[1]Department for Theoretical Physics, Odessa National University, Dvoryanskaya 2, 65026 Odessa, Ukraine
[2]Laboratoire J.A. Dieudonné, UMR 7351 CNRS, Université Nice Sophia Antipolis, Parc Valrose, F-06108 Nice Cedex 02, France

(Received 10 July 2013; revised manuscript received 1 September 2013; published 18 October 2013)

We study the transport properties of a system of active particles moving at constant speed in a heterogeneous two-dimensional space. The spatial heterogeneity is modeled by a random distribution of obstacles, which the active particles avoid. Obstacle avoidance is characterized by the particle turning speed γ. We show, through simulations and analytical calculations, that the mean square displacement of particles exhibits two regimes as function of the density of obstacles ρ_o and γ. We find that at low values of γ, particle motion is diffusive and characterized by a diffusion coefficient that displays a minimum at an intermediate obstacle density ρ_o. We observe that in high obstacle density regions and for large γ values, spontaneous trapping of active particles occurs. We show that such trapping leads to genuine subdiffusive motion of the active particles. We indicate how these findings can be used to fabricate a filter of active particles.

DOI: 10.1103/PhysRevLett.111.160604 PACS numbers: 05.40.Jc, 05.40.Fb, 87.17.Jj

Locomotion patterns are of prime importance for the survival of most organisms at all scales, ranging from bacteria to birds, and often involving complex processes that require energy consumption: i.e., the active motion of the organism [1,2]. The characterization and study of these patterns have a long tradition [1,2] and the experimental observation of subdiffusion, diffusion, and superdiffusion has motivated the development of powerful theoretical tools [3]. It is only in recent years that the (thermodynamical) nonequilibrium nature of these active patterns has been exploited, leading to the study of the so-called active particle systems [4]. Exciting nonequilibrium features have been reported in both interacting as well as noninteracting active particle systems. For instance, large-scale collective motion and giant number fluctuations have been found in interacting active particle systems [5–8]. In noninteracting active particle systems, the presence of active fluctuations leads to complex, nonequilibrium transients in the particle mean square displacement [9,10] and anomalous velocity distributions [11], and the lack of momentum conservation induces nonclassical particle-wall interactions, which allows, for instance, the rectification of particle motion [12–16].

The study of active particle systems has recently witnessed the emergence of a promising new direction: the design and construction of biomimetic, artificial active particles. The directed driving is usually obtained by fabricating asymmetric particles that possess two distinct friction coefficients [17–19], light absorption coefficients [20–23], or catalytic properties [10,24–28] depending on whether energy injection is done through vibration, light emission, or chemical reaction, respectively. One of the most prominent features of these artificial active particles is that their motion is characterized by a diffusion coefficient remarkably larger than the one obtained using symmetric particles [10].

The rapidly expanding study of active particles has focused so far almost exclusively, theoretically as well as experimentally, on the statistical description of particle motion in idealized, homogeneous spaces. However, the great majority of natural active particle systems takes place, in the wild, in heterogeneous media: from active transport inside the cell, which occurs in a space that is filled by organelles and vesicles [29], to bacterial motion, which takes place in highly heterogeneous environments such as the soil or complex tissues such as in the gastrointestinal tract [30]. While diffusion in random media is a well studied subject [31,32], the impact that a

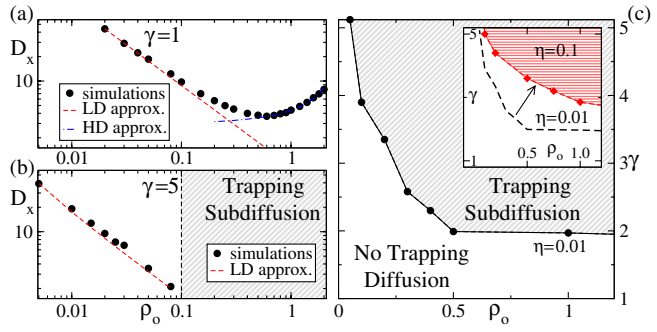

FIG. 1 (color online). Diffusive and subdiffusive regimes. (a) For low values of the turning speed γ, the motion is diffusive and characterized by a diffusion coefficient D_x that exhibits a minimum with the obstacle density ρ_o, as expected by combining the low-density (LD) and high-density (HD) approximation. See Eqs. (9) and (11), and the text. (b) For large values of γ, diffusive motion occurs at low ρ_o values only, while for large ρ_o values particle motion becomes subdiffusive. (c) The boundary between the diffusive and subdiffusive regime is given, for a fixed noise η, by ρ_o and γ (see the inset and Ref. [47]). Parameters: $R = 1$, $L = 100$, $N_p = 10^4$, and $\eta = 0.01$ [$\eta = 0.1$ in the inset of (c)].

heterogeneous medium may have on the locomotion patterns of active particles remains poorly explored.

We address this fundamental problem by using a simple model in which the active organisms move at constant speed in a heterogeneous two-dimensional space, where the heterogeneity is given by a random distribution of obstacles. An "obstacle" may represent the source of a repellent chemical, a light gradient, a burning spot in a forest, or whatever threat that makes our (self-propelled) organisms move away from it once the danger has been sensed, with obstacle avoidance characterized by a (maximum) turning speed γ. Our analysis shows that the same evolution equations (behavioral rules) lead to very different locomotion patterns at low and high density of obstacles. In the dilute obstacle scenario, there is no conflicting information and organisms can easily move away from the undesirable area they find in their way. On the other hand, when we stress the environmental conditions, such that organisms sense several repellent sources simultaneously, the processing of the information is no longer simple. Organisms compute the local obstacle density gradient and use this information to move away from higher obstacle densities. Since the distribution of obstacles is random, as the overall obstacle density increases, this task becomes increasingly more difficult. As a result of this, no strategy guarantees how to escape from obstacles and the organisms behave more and more as if there were no obstacles in the system. For low γ values, we find that the above described change of behavior is reflected by the minimum exhibited by the diffusion coefficient at intermediate obstacle densities ρ_o [see Fig. 1(a)]. For large γ values, particle motion is diffusive at small densities ρ_o, while for large enough densities a new phenomenon emerges: spontaneous trapping of particles [see Fig. 1(b)]. These traps are closed orbits found by the particles in a landscape of obstacles [see Fig. 2]. The time particles spend in these orbits is heavy-tailed distributed, and particle motion is genuinely (i.e., asymptotically) subdiffusive. The boundary between the diffusive and subdiffusive regime depends on γ and ρ_o as illustrated in Fig. 1(c).

Model definition.—We consider a continuum time model for N_p self-propelled particles moving in a two-dimensional space of linear size L where N_o obstacles are placed at random [33]. Boundary conditions are periodic. In the over-damped limit, the equations of motion of the ith particle are given by

$$\dot{\mathbf{x}}_i = v_0 \mathbf{V}(\theta_i), \tag{1}$$

$$\dot{\theta}_i = h(\mathbf{x}_i) + \eta \xi_i(t), \tag{2}$$

where the dot denotes the temporal derivative, $\mathbf{x}_i$ corresponds to the position of the ith particle, and θ_i corresponds to its moving direction. The function $h(\mathbf{x}_i)$ represents the interaction with obstacles and its definition is given by

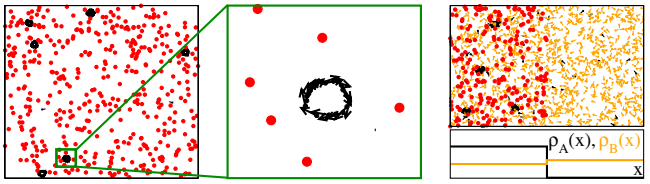

FIG. 2 (color online). Trapping and filtering. Left: for large values of γ and ρ_o, spontaneous trapping of particle occurs (see the Supplemental Material [45]). Obstacles are indicated by red dots while black arrows correspond to active particles with $\gamma = 5$. Right: by placing obstacles on the left half of the box, particles with $\gamma_A = 5$ (black) are confined to this region, while particles with $\gamma_B = 1$ (orange) diffuse freely over the system. Parameters: $\rho_o = 0.5$, $\eta = 0.01$, and $L = 30$.

$$h(\mathbf{x}_i) = \begin{cases} \frac{\gamma}{n(\mathbf{x}_i)} \sum_{\Omega_i} \sin(\alpha_{k,i} - \theta_i) & \text{if } n(\mathbf{x}_i) > 0 \\ 0 & \text{if } n(\mathbf{x}_i) = 0, \end{cases} \tag{3}$$

where the sum runs over all neighboring obstacles Ω_i such that $0 < |\mathbf{x}_i - \mathbf{y}_k| < R$, with $\mathbf{y}_k$ the position of the kth obstacle and $n(\mathbf{x}_i)$ the cardinal number of Ω_i. The term $\alpha_{k,i}$ is the angle, in polar coordinates, of the vector $\mathbf{x}_i - \mathbf{y}_k$. In Eq. (1), v_0 is the active particle speed and $\mathbf{V}(\theta) \equiv (\cos(\theta), \sin(\theta))^T$. The additive white noise in Eq. (2) is characterized by an amplitude η and obeys $\langle \xi_i(t) \rangle = 0$ and $\langle \xi_i(t) \xi_j(t') \rangle = \delta_{i,j} \delta(t - t')$, which leads to an angular diffusion $D_\theta = \eta^2/2$. Notice that for $\gamma = 0$, Eqs. (1) and (2) define a system of persistent random walkers characterized by a diffusion coefficient $D_{x_o} = v_0^2/(2D_\theta)$ (see Refs. [1,2,9]).

Continuum description.—We look for a coarse-grained description of the system in terms of the concentration $p(\mathbf{x}, \theta, t)$ of particles at position $\mathbf{x}$ and orientation θ at time t. The evolution of $p(\mathbf{x}, \theta, t)$ obeys [35]

$$\partial_t p + v_0 \nabla \cdot [\mathbf{V}(\theta) p] = D_\theta \partial_{\theta\theta} p + F[p(\mathbf{x}, \theta, t), \rho_o(\mathbf{x})], \tag{4}$$

where D_θ is the angular diffusion as defined above, and $F[p(\mathbf{x}, \theta, t), \rho_o(x)]$ represents the interaction of the self-propelled particles with the obstacles. The term $\rho_o(\mathbf{x})$ refers to the obstacle density at position $\mathbf{x}$ [36]. Here, we discuss two clear limits where $F[p(\mathbf{x}, \theta, t), \rho_o(x)]$ can be specified. We refer to these limits as the low-density (LD) and high-density (HD) (obstacle) approximation.

Low-density approximation.—We consider that the active particles move most of the time freely, bumping into obstacles only occasionally. More specifically, we assume that η, $\rho_o \ll 1$ and approximate the interaction with obstacles, for time scales much larger than $2R/v_0$, as sudden changes in the moving direction of the particle. Let $T(\theta, \theta'; \mathbf{x})$ be the rate at which a particle at position $\mathbf{x}$ and moving in direction θ turns into direction θ'. To compute $T(\theta, \theta'; \mathbf{x})$ we need to estimate the frequency at which particles encounter obstacles as well as the scattered

angle after each obstacle interaction. If $D_\theta^{-1} v_0 \gg \rho_o^{-1/2}$, we can approximate particle motion, in between successive encounters with obstacles, as ballistic. In this limit, the obstacle encounter rate can be estimated as $\lambda(\rho_o) \approx v_o \rho_o \sigma_o$, where $\sigma_o = 2R$. To simplify the calculations we approximate the scattered angle distribution by a simple top-hat functional form. Putting all this together, we express $T(\theta, \theta'; \mathbf{x}) \simeq \lambda(\rho_o) T(\theta, \theta') \approx [\lambda(\rho_o)/(2\epsilon_\theta)]\Theta(\epsilon_\theta - |\theta - \theta'|)$ and write F as

$$F[p] = -\lambda(\rho_o) p(x, \theta, t) + \int_0^{2\pi} d\theta' T(\theta, \theta') p(x, \theta', t) \approx \frac{\lambda(\rho_o)\epsilon_\theta^2}{6} \partial_{\theta\theta} p, \quad (5)$$

where ϵ_θ is numerically obtained from the study of the scattering process. Expression (5) allows us to rewrite the rhs of Eq. (4) as $\tilde{\mathcal{D}}_\theta \partial_{\theta\theta} p$, where $\tilde{\mathcal{D}}_\theta$ is defined as $\tilde{\mathcal{D}}_\theta = D_\theta + \lambda(\rho_o)\epsilon_\theta^2/6$. By performing a moment expansion of Eq. (4), where we define $\rho(\mathbf{x}, t) = \int d\theta p$, $P_x(\mathbf{x}, t) = \int d\theta \cos(\theta) p$, $P_y(\mathbf{x}, t) = \int d\theta \sin(\theta) p$, and $Q_s(\mathbf{x}, t) = \int d\theta \sin(2\theta) p$, and $Q_c(\mathbf{x}, t) = \int d\theta \cos(2\theta) p$, we arrive at the following set of equations:

$$\partial_t \rho = -v_0 \nabla \cdot \mathbf{P}, \quad (6)$$

$$\partial_t P_x = -\frac{v_0}{2} \nabla \cdot [Q_c + \rho, Q_s] - \tilde{\mathcal{D}}_\theta P_x, \quad (7)$$

$$\partial_t P_y = -\frac{v_0}{2} \nabla \cdot [Q_s, \rho - Q_c] - \tilde{\mathcal{D}}_\theta P_y, \quad (8)$$

where we assumed that $\partial_t Q_c = \partial_t Q_s = 0$. It can be shown that the temporal evolution of Q_c and Q_s is faster than the one of P_x and P_y, which in turn is faster than the one for ρ. Since we are interested in the long-time behavior of $\rho(\mathbf{x}, t)$, and there is no induced order, we take $Q_c = Q_s = 0$ and use the fast relaxation of Eqs. (7) and (8) to express P_x and P_y as slave functions of ρ and its derivatives [37]. This procedure leads to the following asymptotic equation for $\rho(\mathbf{x}, t)$:

$$\partial_t \rho = \nabla \cdot \left[\frac{v_0^2}{2\tilde{\mathcal{D}}_\theta} \nabla \rho\right]. \quad (9)$$

From Eq. (9), it is evident that the spatial diffusion coefficient D_x takes the form $D_x = v_0^2/[2(D_\theta + \Lambda_0 \rho_o)]$, with $\Lambda_0 = v_0 \sigma_0 \epsilon_\theta^2/6$. Notice that D_x is a decreasing function of ρ_o [38].

High-density approximation.—At large obstacle densities, particles always sense the presence of several obstacles around them. This means that we cannot think of collisions as rare sudden jumps in the moving direction. Thus, we replace Eq. (5) with a direct, local, coarse-grained expression for the interactions. This means that we leave the Boltzmann for the Fokker-Planck approach where the interaction with obstacles is expressed by $F = \partial_\theta[I p(\mathbf{x}, \theta, t)]$. The term I represents the (average) interaction felt by a particle at $\mathbf{x}$ moving in direction θ, which takes the form

$$I = \frac{\gamma}{n(\mathbf{x})} \sum_j \sin(\theta - \alpha_j) = \frac{\gamma \Gamma(\mathbf{x})}{n(\mathbf{x})} \sin(\theta - \psi(\mathbf{x})), \quad (10)$$

where j is an index that runs over all neighboring obstacles, α_j is the polar angle associated with the vector $\mathbf{x} - \mathbf{y}_j$, and $\Gamma(\mathbf{x})$ and $\psi(\mathbf{x})$ are the modulus and phase, respectively, of $\sum_j \exp(\imath(\alpha_j))$ (see Ref. [40]). We now approximate Eq. (10) by its average and use the fact that it represents a sum of n random vectors of magnitude 1 in the complex plane, to express $I \sim \sin(\theta - \psi(\mathbf{x}))/\sqrt{n}$, where $n \approx \pi R^2 \rho_o$. Inserting this approximated expression into Eq. (4) and performing the moment expansion and approximations that led us from Eqs. (6)–(8) to Eq. (9), we arrive at

$$\partial_t \rho = \frac{v_0^2}{2D_\theta} \nabla^2 \rho - \frac{\gamma v_0}{2D_\theta R\sqrt{\pi\rho_0}} \nabla \cdot [(\cos(\psi), \sin(\psi))\rho] = D_{x_o} \nabla^2 \rho - \frac{\gamma v_0}{2D_\theta R\sqrt{\pi\rho_0}} \nabla \cdot \left[\frac{\rho \nabla \rho_o(\mathbf{x})}{\| \nabla \rho_o(\mathbf{x}) \|}\right], \quad (11)$$

where we have approximated the vector field $(\cos(\psi), \sin(\psi)) \sim \nabla\rho_o(\mathbf{x})/\| \nabla\rho_o(\mathbf{x}) \|$. If we replace our current definition of ρ by a local average over a volume of linear dimensions much larger than R and look for the long-time dynamics of this redefined density, by applying homogenization techniques, we expect to recover a diffusive behavior with a new effective diffusion, whose explicit form depends on the statistical properties of the random field $\rho_o(\mathbf{x})$ and is proportional to the square of the constant in front of the convective term. While according to Eq. (9) (LD approximation), $D_x \to 0$ as $\rho_o \to \infty$, Eq. (11) (i.e., the HD approximation) indicates that in the limit of $\rho_o \to \infty$, $D_x \to D_{x0}$, where D_{x0} is the diffusion coefficient in the absence of obstacles defined above. These two results necessarily imply the existence of a minimum in the spatial diffusion coefficient D_x as ρ_o is increased from 0 to ∞. Moreover, this minimum has to be located at the crossover between the LD and HD approximation, which can be roughly estimated to occur at $\rho_c \sim 1/(\pi R^2)$, around which $D_x \sim 1/[\rho_c - \Lambda_1 \rho_o]$, with Λ_1 a constant. All these findings are confirmed by particle simulations as shown in Fig. 1.

Trapping.—Equation (11) indicates that the vector field $\nabla\rho_o(\mathbf{x})$ governs the long-term dynamics at high obstacle concentrations. In particular, the random distribution of obstacles, together with the compressible nature of $\rho(\mathbf{x}, t)$, may result in the spontaneous formation of active particle sinks. These topological defects, which we refer to as "traps," are indeed observed in simulations for large values of γ (see Fig. 2). Inside traps particles form vortex-like patterns. The average time $\langle \tau_T \rangle$ spent by a particle inside a trap depends on the precise configuration of the obstacles that form the trap. We find that the presence of traps can lead to a genuine subdiffusive behavior, with

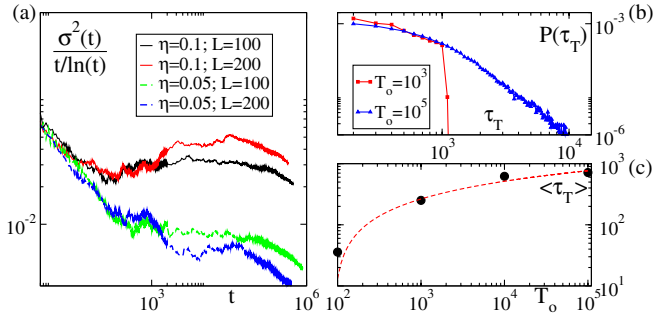

FIG. 3 (color online). Genuine subdiffusive behavior. (a) Scaling of the mean square displacement $\sigma^2(t)$ with t for two system sizes, with $N_p/L^2 = 1$, $\rho_o = 0.5$, and $\gamma = 5$. (b) The distribution of trapping times $P(\tau_T)$ is power-law distributed for long enough T_o. (c) The average waiting time $\langle \tau_T \rangle$ is an increasing function of T_o. The red dashed curve corresponds to a fit $\propto \ln(T_o)$. Measurements in (b) and (c) were performed on a particular trap for $\eta = 0.1$.

particles exhibiting a mean square displacement $\sigma^2(t) = \langle \mathbf{x}^2(t) \rangle$ that grows slower than t. To test this observation, let us assume that particle motion can be conceived as a random walk across a two-dimensional array of traps such that $\sigma^2(t) \propto n_J(t)$, where $n_J(t)$ represents the number of jumps from trap to trap the random walker performs during t. To estimate $n_J(t)$, we study the distribution to trapping times $P(\tau_T)$ of a given trap [see Fig. 3(b)]. Subdiffusion can only occur if $P(\tau_T)$ is asymptotically power-law distributed and such that $\langle \tau_T \rangle$ grows with the observation time T_o as $\ln(T_o)$ or faster [39] [see Figs. 3(b) and 3(c)]. Within this simplified picture, the behavior of $\langle \tau_T \rangle$ shown in Fig. 3(c) suggests that $\sigma^2(t) \propto n_J(t) \sim t/\ln(t)$. By taking $t \to \infty$, we expect $\sigma^2(t)/[t/\ln(t)]$ to approach a constant value. Figure 3(a) clearly shows that $\sigma^2(t)$ is slower than $t/\ln(t)$. Arguably, this is due to the fact that once a particle escapes from a trap, typically it performs a small excursion before being reabsorbed by the same trap.

Discussion.—The spontaneous trapping of particles depends not only on ρ_o but also on γ, which is an intrinsic property of the particle. This means that given the same spatial environment, two particle types, say characterized by γ_A and γ_B, will respond differently. We can make use of this fact to fabricate a simple and cheap filter as indicated in Fig. 2 (right). Notice that trapping of one of the particle types is required to obtain this effect.

Trapping, rectification, and sorting have been reported for a particular kind of active particles: chiral, i.e., circularly moving particles [41,42]. By placing L-shaped obstacles on a regular lattice, the motion of such particles can be rectified [42], while elongated obstacles arranged in flowerlike patterns can be used to selectively trap either levogyre or dextrogyre particles [41]. For nonchiral active particles, trapping and rectification can be achieved by using V-shape objects. Kaiser *et al.* in Refs. [43,44] showed that self-propelled rods can be trapped by placing V-shape objects. These traps provide a geometrical constraint to the active particles that end up being blocked in the V-shape devices. On the other hand, by arranging in line V-shape objects, but with their tips open, rectification of particle motion can be achieved [12,15]. Notice that these V-shape objects, either with their tip closed or opened, cannot be used to produce a filter of active particles. On the other hand, the novel trapping and sorting mechanism reported here is generic and should apply to all kinds of active particles, including interacting, noninteracting, chiral, or nonchiral active particles.

Finally, it is important to mention that genuine subdiffusion occurs for fixed obstacles only. For slowly diffusing obstacles the asymptotic behavior of the active particles is diffusive. Interestingly, trapping and subdiffusive behavior is also observed for aligning self-propelled particles as those studied in [34] for values of the interaction strength significantly smaller than those associated with obstacle avoidance (see the Supplemental Material [45]).

Our results open a new route to control active particle systems. For instance, we believe that simple experimental realizations of the described dynamics could be achieved by placing phototactic organisms on arenas with distributions of bright and dark spots. Specifically, we speculate that for *Chlamydomonas Reinhardtii* [46] a change of behavior might occur by varying R between 50 and 250 μm at $\rho_o \sim 0.3$.

Numerical simulations have been performed at the 'Mesocentre SIGAMM' machine, hosted by Observatoire de la Côte d'Azur. We thank F. Delarue and R. Soto for valuable comments on the manuscript and the Fed. Doeblin for partial financial support.

*Peruani@unice.fr

[1] H. Berg, *Random Walks in Biology* (Princeton University, Princeton, NJ, 1983).
[2] A. Okubo and S. Levin, *Diffusion and Ecological Problems* (Springer, New York, 1980).
[3] R. Metzler and J. Klafter, Phys. Rep. **339**, 1 (2000).
[4] P. Romanczuk, M. Bär, W. Ebeling, B. Lindner, and L. Schimansky-Geier, Eur. Phys. J. Special Topics **202**, 1 (2012).
[5] T. Vicsek and A. Zafeiris, Phys. Rep. **517**, 71 (2012).
[6] S. Ramaswamy, Annu. Rev. Condens. Matter Phys. **1**, 323 (2010).
[7] F. Peruani, J. Starruß, V. Jakovljevic, L. Søgaard-Andersen, A. Deutsch, and M. Bär, Phys. Rev. Lett. **108**, 098102 (2012).
[8] F. Ginelli, F. Peruani, M. Bär, and H. Chaté, Phys. Rev. Lett. **104**, 184502 (2010).
[9] F. Peruani and L. G. Morelli, Phys. Rev. Lett. **99**, 010602 (2007).
[10] R. Golestanian, Phys. Rev. Lett. **102**, 188305 (2009).
[11] P. Romanczuk and L. Schimansky-Geier, Phys. Rev. Lett. **106**, 230601 (2011).

[12] P. Galajda, J. Keymer, P. Chaikin, and R. Austin, J. Bacterial. **189**, 8704 (2007).
[13] H. H. Wensink and H. Löwen, Phys. Rev. E **78**, 031409 (2008).
[14] M. B. Wan, C. J. Olson Reichhardt, Z. Nussinov, and C. Reichhardt, Phys. Rev. Lett. **101**, 018102 (2008).
[15] J. Tailleur and M. Cates, Europhys. Lett. **86**, 60002 (2009).
[16] P. K. Radtkeand L. Schimansky-Geier, Phys. Rev. E **85**, 051110 (2012).
[17] A. Kudrolli, G. Lumay, D. Volfson, and L. Tsimring, Phys. Rev. Lett. **100**, 058001 (2008).
[18] J. Deseigne, O. Dauchot, and H. Chaté, Phys. Rev. Lett. **105**, 098001 (2010).
[19] C. A. Weber, T. Hanke, J. Deseigne, S. Léonard, O. Dauchot, E. Frey, and H. Chaté, Phys. Rev. Lett. **110**, 208001 (2013).
[20] H.-R. Jiang, N. Yoshinaga, and M. Sano, Phys. Rev. Lett. **105**, 268302 (2010).
[21] R. Golestanian, Phys. Rev. Lett. **108**, 038303 (2012).
[22] I. Theurkauff, C. Cottin-Bizonne, J. Palacci, C. Ybert, and L. Bocquet, Phys. Rev. Lett. **108**, 268303 (2012).
[23] J. Palacci, S. Sacanna, A. P. Steinberg, D. J. Pine, and P. M. Chaikin, Science **339**, 936 (2013).
[24] W. Paxton, K. C. Kistler, C. C. Olmeda, A. Sen, S. K. St. Angelo, Y. Cao, T. E. Mallouk, P. E. Lammert, and V. H. Crespi, J. Am. Chem. Soc. **126**, 13 424 (2004).
[25] N. Mano and A. Heller, J. Am. Chem. Soc. **127**, 11 574 (2005).
[26] G. Rückner and R. Kapral, Phys. Rev. Lett. **98**, 150603 (2007).
[27] J. Howse, R. Jones, A. Ryan, T. Gough, R. Vafabakhsh, and R. Golestanian, Phys. Rev. Lett. **99**, 048102 (2007).
[28] R. Golestanian, T. B. Liverpool, and A. Ajdari, Phys. Rev. Lett. **94**, 220801 (2005).
[29] B. Alberts *et al.*, *Molecular Biology of the Cell* (Garland Science, New York, 1994).
[30] *Myxobacteria II*, edited by M. Dworkin and D. Kaiser (ASM Press, Herndon, VA, 1993).
[31] J.-P. Bouchaud and A. Geoges, Phys. Rep. **195**, 127 (1990).
[32] H. Berry and H. Chaté, arXiv:1103.2206.
[33] Collective effects of an interacting version of this model were studied in Ref. [34]. Here, we focus on individual locomotion patterns.
[34] O. Chepizhko, E. G. Altmann, and F. Peruani, Phys. Rev. Lett. **110**, 238101 (2013).
[35] C. W. Gardiner, *Handbook of Stochastic Methods* (Springer-Verlag, Berlin, 2004).
[36] We reserve the symbol ρ_o, without $\mathbf{x}$ dependency, to the global obstacle density.
[37] Alternatively, multiscaling analysis can be used to go from Eqs. (4) and (5) to Eq. (9).
[38] There are qualitative differences with the Lorentz gas model (see Ref. [39]). Here, angular diffusion acts on the moving particles in between collisions. On the other hand, the scattering process is remarkably different due to the absence of conserved quantities.
[39] P. L. Krapivsky, S. Redner, and E. Ben-Naim, *A Kinetic View of Statistical Physics* (Cambridge University Press, Cambridge, England, 2010).
[40] Y. Kuramoto, in *International Problems in Theoretical Physics*, Lecture Notes in Physics, edited by H. Araki (Springer, New York, 1975).
[41] M. Mijalkov and G. Volpe, Soft Matter **9**, 6376 (2013).
[42] C. Reichhardt and C. J. Olson Reichhardt, arXiv:1307.0755.
[43] A. Kaiser, H. H. Wensink, and H. Löwen, Phys. Rev. Lett. **108**, 268307 (2012).
[44] A. Kaiser, K. Popowa, H. H. Wensink, and H. Löwen, Phys. Rev. E **88**, 022311 (2013).
[45] See Supplemental Material at http://link.aps.org/supplemental/10.1103/PhysRevLett.111.160604 for movies.
[46] M. Garcia, S. Berti, P. Peyla, and S. Rafaï, Phys. Rev. E **83**, 035301 (2011).
[47] The boundary was estimated (i) by measuring $D_x(t \to \infty) = \langle \mathbf{x}^2(t) \rangle / 4t$, and (ii) by estimating when the asymptotic fraction of particles on the left half of the box in systems prepared as indicated in Fig. 2 (right) was above 0.5. Both methods led to the same boundary estimate.